

## A theoretical study on quadrupole coupling parameters of HRPII protein modeled as $3_{10}$ -helix & $\alpha$ -helix structures

Fatemeh Elmi<sup>a,\*</sup>, Nasser L. Hadipour<sup>b</sup>

<sup>a</sup>Faculty of Marine & Oceanic Sciences, Department of Marine Chemistry, University of Mazandaran, P.O. BOX: 47416-9544, Babolsar, Iran

<sup>b</sup>Department of Chemistry, Tarbiat Modares University, P.O. BOX: 82883455, Tehran, Iran

Received: 13 April 2016, Accepted: 30 August 2016, Published: 30 August 2016

### Abstract

A fragment of Histidine rich protein II (HRP II 215-236) was investigated by  $^{14}\text{N}$  and  $^{17}\text{O}$  electric field gradient, EFG, tensor calculations using DFT. This study intends to explore the differences between  $3_{10}$ -helix and  $\alpha$ -helix of HRPII both in the gas phase and in solution. To achieve the aims, the  $^{17}\text{O}$  and  $^{14}\text{N}$  NQR parameters of a fragment of HRPII (215-236) for both structures are calculated. Due to the side chain arrangements of the  $3_{10}$ -helix, this conformation contains several hydrogen bonding contacts in comparison to the  $\alpha$ -helix form. The resultant  $^{14}\text{N}$  and  $^{17}\text{O}$   $\chi, \eta$  s of peptide bonds of HRPII are affected by these contacts. Both in the gas phase and in solution, the differences in  $^{14}\text{N}$   $\chi, \eta$  s of backbone are within the uncertainties identical between two conformers but not for NH groups of backbone whose related amino acids participate in intramolecular hydrogen bond formation with side chain. In this case, the differences in  $^{14}\text{N}$   $\chi$  s of backbone are  $\Delta\chi_{\text{avg.}} = 0.36$  in gas phase and  $\Delta\chi_{\text{avg.}} = 0.43\text{MHz}$  in solution. However, differences in  $^{17}\text{O}$   $\chi, \eta$  parameters of the backbone C=O are distinguishable between two conformers, regardless of in gas phase and in solution, with and without influencing of the intramolecular hydrogen bond. These differences reveal how hydrogen bond interactions affect EFG tensors at the sites of oxygen and nitrogen nuclei.

**Keywords:** Histidine rich protein II;  $^{17}\text{O}$  and  $^{14}\text{N}$  NQR; DFT; hydrogen bond.

### Introduction

Understanding protein structure is one of the most important goals of modern biophysics. Accurate determination of proteins conformation is a formidable task. However, based on the study of small peptides, theoretical calculations can provide a basis for understanding protein structure. In bio-macromolecules such as peptides, proteins, and carbohydrates, carbonyl

oxygen and amide nitrogen play an important role in molecular conformations, for instance through hydrogen bonding [1]. Although NMR parameters are very useful in determination of protein structures, combination with nuclear quadrupole resonance (NQR) parameters can reveal a better interpretation of the observed results. Nuclear quadrupole coupling constant,  $\chi$ , and asymmetry parameter,

\*Corresponding author: Fatemeh Elmi

Tel: +98 (11) 35302921, Fax: +98 (11) 35302921  
E-mail: f.elmi@umz.ac.ir

$\eta$  are those experimentally measurable NQR parameters. The value of  $\chi$  is proportional to electric field gradient, EFG, tensor whereas  $\eta$  indicates the deviation of EFG tensors from axial symmetry.

In this study, calculation of NQR parameters are used to study a repeating sequence of malaria biomarker, histidine rich protein II (HRP II 215-236) in both  $3_{10}$ -helix and  $\alpha$ -helix forms. It mainly consists of His and Ala residues totally 76 % and 11% Asp residue [2-4]. The most repeated sequence of HRP II is AHH, AHHAAD, and HHAHHAAD. However, the exact structure of HRPII is not completely known. There is only one theoretical model for HRPII in protein data bank which indicates that this protein is mainly composed of 18  $\alpha$ -helices [5]. However, the circular dichroism (CD) spectroscopy results show that HRPII undergoes large secondary structure changes from random coil for free protein to the structure that resembles the  $3_{10}$ -helix for HRPII-heme complex [6]. However, there is no strong evidence that HRPII structure changes to  $3_{10}$ -helix or  $\alpha$ -helix upon heme binding [7-9]. Several studies reveal that a repetitive hexapeptide sequence AHHAAD within the HRPII protein is responsible for binding to multiple heme molecules which detoxify the toxic free heme in malaria life cycle [10-12]. The two hexapeptide repeating sequence of HRPII was studied *via* molecular dynamics (MD) simulation in water at 300K with  $\alpha$ -helix as initial structure. The results showed that the repeating sequence loses its initial  $\alpha$ -helix structure rapidly and is converted to random coil and bent secondary structures [13]. In addition,  $^{17}\text{O}$  NQR parameters of backbone carbonyl

oxygen are explored on initial  $\alpha$ -helix and final random coil and bent secondary structures. The results indicate that quadrupole coupling constants show a significant sensitivity to the hydrogen bond interactions in peptide. In this work, a 22 amino acid fragment of HRPII, with HATDAHHAADAHHAADAHHATD sequence modeled as  $3_{10}$ -helix and  $\alpha$ -helix structures is studied (Figure1). This sequence contains two hexapeptide and one tripeptide repeating sequence of HRPII.

The hydrogen bonds are very sensitive to the secondary structures of proteins and polypeptides. They are used as critical indicators of the existing different types of helices and  $\beta$ -sheets. Due to the difficulties in experimentally distinguishing between the  $\alpha$ -helix and  $3_{10}$ -helix conformers, we have conducted a theoretical study which delineates the differences between two conformers both in the gas phase and in solution. In order to elucidate the influence of peptide conformation on  $^{17}\text{O}$  and  $^{14}\text{N}$  NQR parameters which contribute in the  $\text{CO}^{14}\text{NH}\dots^{17}\text{O} = \text{CNH}$  type of hydrogen bond, density functional theory (DFT) calculations were performed for both  $\alpha$ -helix and  $3_{10}$ -helix structures. As a result of the formation of a hydrogen bond in a conformer, the quadrupolar nuclei of the conformer feel the changes in the EFG tensor, which is reflected in the calculated NQR parameters. The results are given in Tables 1-4. The NQR results of  $^{17}\text{O}$  and  $^{14}\text{N}$  of the peptide backbone predict that the  $^{17}\text{O}$  NQR would be a more feasible technique to distinguish between these two conformers both in the gas phase and in solution.

### Computational details

Quantum chemical methods could provide all of the long range interactions (hydrogen bonds, dipole-dipole interactions, etc.). Such interactions influence the secondary structure of proteins and polypeptides. DFT has emerged as the most effective quantum chemical tools to study the systems large enough to exhibit significant long-range interactions. Based on the solvent effect, a solvent model has been selected in this study, the polarizable continuum model (PCM) [14]. It includes a solvent reaction field self-consistent with the solute electrostatic potential. Water

with a dielectric constant ( $\epsilon=78.4$ ) was selected as the main solvent. All of the EFG calculations are carried out using DFT in Gaussian 98 package and prop keyword [15]. We have used 6-311++G\*\* basis set and Becke's three-parameter functional [16] with a nonlocal correlation term given by the Lee, Yang, and Parr expression [17], and the B3LYP hybrid exchange-correlation functional. Several studies indicated that the employed method and basis set yield reliable results in studying the effect of hydrogen bonds on NQR parameters in such systems [18-23].

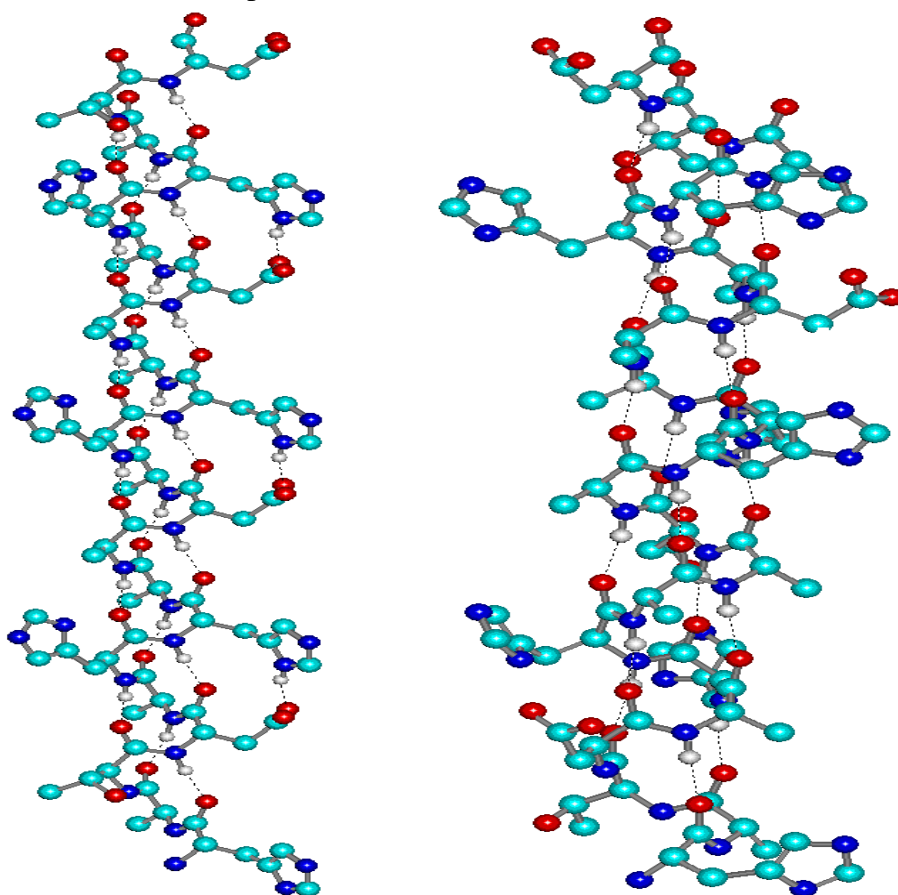


**Figure 1.** A fragment of HRPII(HATDAHHAADAHHAADAHHATD) peptide in both  $3_{10}$ -helix (a) and  $\alpha$ -helix (b) forms

## Theory

NQR has proved to be an efficient method to distinguish between different conformers [24]. Quadrupolar nuclei ( $I > 1/2$ ) are associated with nuclear quadrupole coupling constants,  $\chi$ s according to equation:

$$\chi = \frac{e^2 Q q_{zz}}{h} \quad (1)$$

Where  $e, h$  and  $Q$  are the unit of electrostatic charge, plank constant, and electric quadrupole moment, respectively. The value of  $\chi$  is proportional to EFG tensor which originates from the internal electrostatic charges at the site of the quadrupolar nucleus [25]. The EFG tensor can be expressed in the principal axis system (PAS) in which it is diagonalized. EFG tensor is traceless, i.e:

$$V_{xx} + V_{yy} + V_{zz} = 0 \quad (2)$$

So by convention, it can be expressed in terms of two quantities,

$$eq_{zz} = V_{zz} = \frac{\partial^2 V}{\partial z^2} \quad (3)$$

and

$$\eta = \left| \frac{V_{xx} - V_{yy}}{V_{zz}} \right|, \quad 0 \leq \eta \leq 1 \quad (4)$$

[19]. Electric quadrupole moments of  $^{14}\text{N}$  ( $I=1$ ) and  $^{17}\text{O}$  ( $I=5/2$ ) are taken as  $Q = 20.44 \times 10^{-27} \text{ cm}^2$  and  $Q = -25.58 \times 10^{-27} \text{ cm}^2$ , respectively [26].

## Results and discussion

Figure 1 shows the differences between the two structures. Conversion of  $\alpha$ -helix into the  $3_{10}$ -helix form leads to changes in the size of  $\psi$  and  $\phi$  torsion angles which is accompanied by  $(i/i+4) \rightarrow (i/i+3)$  sequential transformation in peptide bonds. The

average N-O distances between two H-bonded residues are 3.02 Å and 2.85 Å in  $\alpha$ -helix and  $3_{10}$ -helix forms, respectively. Also, the average N-H-O bond angles are 175° in  $3_{10}$ -helix and 169° in  $\alpha$ -helix forms. The  $3_{10}$ -helix structure allows several changes in structural parameters. For example, as it is shown in  $\alpha$ -helix structure, there is no side chain HBs. In contrast, there are three side chain HBs in  $3_{10}$ -helix structure for this fragment. These HBs are formed by NH groups of imidazole ring, a constituent of numbers 7,13, and 19 His residues and the CO groups of adjacent Asp residues. The geometric parameters of these three HBs are almost the same. The N-O bond length is 2.68 Å and the N-H-O bond angle is 160°. However, this conversion of  $\alpha$ -helix into the  $3_{10}$ -helix along with formation of side chain hydrogen-bonding causes redistribution of electronic charges in the HRPII monomer. This redistribution of charges introduces changes in peptide bond lengths and peptide bond angles. These alterations may be better seen in NQR parameters of  $^{14}\text{N}$  and  $^{17}\text{O}$  nuclei. The effects on  $\chi, \eta$ s of  $^{14}\text{N}$  and  $^{17}\text{O}$  are briefly explained here. One should note that in  $\eta$ , the three diagonal components,  $q_{xx}, q_{yy}$ , and  $q_{zz}$  of the EFG tensors are involved. So, a small fractional shift in one of the EFG components makes a large variation in the asymmetry parameter. In contrast,  $\chi$  only contains  $q_{zz}$ , which possess much smaller uncertainties than  $\eta$ . Due to the side chain arrangements of the  $3_{10}$ -helix, this conformation contains several hydrogen bonding contacts in comparison to the  $\alpha$ -helix form. The resultant  $^{14}\text{N}$  and  $^{17}\text{O}$   $\chi, \eta$ s of peptide bonds are affected by these contacts. To gain insight into the factors determining

the  $^{14}\text{N}$  and  $^{17}\text{O}$   $\chi$  differences, it is worthy to note that each hydrogen bond can be considered as a large induced dipole. The induced dipoles are not only generated by primary hydrogen bonding interactions but also by space electrostatic interactions *via* the partial atomic charges of hydrogen, nitrogen and oxygen atoms which belong to different hydrogen bond network [27]. This phenomenon brings about redistribution of electronic charges around each quadrupolar site which can

be seen in the values of  $^{17}\text{O}$  and  $^{14}\text{N}$  NQR parameters. Table 1 shows the calculated  $^{14}\text{N}$  NQR parameters for both  $\alpha$ -helix and  $3_{10}$ -helix structures. The differences in  $^{14}\text{N}$   $\chi, \eta$ s of backbone are within the uncertainties identical between two conformers,  $\Delta\chi_{\text{avg.}}=0.20$  MHz,  $\Delta\eta_{\text{avg.}}=0.07$ . It is notable that the type of residue has no significant effect on NQR parameter of the main chain atoms [13,28].

**Table 1.**  $^{14}\text{N}$  NQR parameters of peptide backbone of a fragment of HRPII

Nuclei	$3_{10}$ -helix		$\alpha$ -helix		$ \Delta\chi ^{\text{MHz}}$	$ \Delta\eta $
	$\chi^{\text{MHz}}$	$\eta$	$\chi^{\text{MHz}}$	$\eta$		
N-Asp1	4.10	0.24	4.30	0.14	0.20	0.1
N-His2	4.0	0.32	4.22	0.22	0.22	0.1
N-His3	3.6	0.39	4.02	0.22	0.42	0.17
N-Ala4	3.87	0.33	4.17	0.23	0.30	0.1
N-Ala5	3.91	0.32	4.07	0.27	0.16	0.05
N-Asp6	3.80	0.36	3.90	0.27	0.10	0.09
N-Ala7	3.90	0.35	4.01	0.28	0.11	0.07
N-His8	3.92	0.39	4.11	0.32	0.19	0.07
N-His9	3.64	0.43	3.98	0.28	0.34	0.15
N-Ala10	3.79	0.36	4.08	0.27	0.29	0.09
N-Ala11	3.90	0.34	4.03	0.30	0.13	0.04
N-Asp12	3.83	0.37	3.98	0.31	0.15	0.06
N-Ala13	3.87	0.35	3.94	0.29	0.07	0.06
N-His14	3.93	0.39	4.10	0.32	0.17	0.07
N-His15	3.78	0.42	4.09	0.33	0.31	0.09
N-Ala16	3.76	0.36	4.25	0.29	0.49	0.07

However, the differences are significant for NH backbone of His-7, His-13, and His-19 which the amino site of imidazole ring in  $3_{10}$ -helix structure participates in intramolecular hydrogen bond. In this case, the differences in  $^{14}\text{N}$   $\chi, \eta$ s of backbone between two structures are  $\Delta\chi_{\text{avg.}}=0.36$  MHz, and  $\Delta\eta_{\text{avg.}}=0.14$ . To assess the solvent effect, PCM is also applied for both structures. As seen from Table 2, the calculated average  $^{14}\text{N}$   $\chi$  in solution which should provide a more accurate prediction than the gas-phase results for the signals in HRPII protein to be

defined in future experiments, are  $\chi_{\text{avg.}, \alpha\text{-helix}}=3.95$  MHz and  $\chi_{\text{avg.}, 3_{10}\text{-helix}}=3.48$  MHz. It should be noted that the calculated differences in  $^{14}\text{N}$   $\chi, \eta$ s of backbone between  $\alpha$ -helix and  $3_{10}$ -helix structures in solution are  $\Delta\chi_{\text{avg.}}=0.22$  MHz and  $\Delta\eta_{\text{avg.}}=0.10$ . The same as in gas phase, the differences are significant for NH backbone of His-7, His-13, and His-19 whose imidazole residue in  $3_{10}$ -helix structure takes part in intramolecular hydrogen bond. In this case, the differences in  $^{14}\text{N}$   $\chi, \eta$ s of backbone between two structures are  $\Delta\chi_{\text{avg.}}=0.43$  MHz, and  $\Delta\eta_{\text{avg.}}=0.09$ . The

average differences between  $^{14}\text{N}$   $\chi$  of backbone between gas phase and solution for  $\alpha$ -helix and  $3_{10}$ -helix are  $\Delta\chi_{\text{avg.}} = 0.37$  MHz and  $0.41$  MHz, respectively. Moreover, absolute  $\chi$  values slightly decreased from gas phase to solution. For both  $\alpha$ -helix and  $3_{10}$ -helix structures, calculated  $^{17}\text{O}$  NQR parameters for backbone oxygen atoms are depicted in Table 3. The calculated average  $^{17}\text{O}$   $\chi$  is  $9.63$  MHz for  $\alpha$ -helix structure which is fairly consistent with those experimentally determined by Takahashi *et al.* [29],  $\chi$ ,  $\text{exp}(^{17}\text{O}) = 9.28$  MHz, and the theoretical value calculated by Torrent *et al.* [28],  $\chi$  ( $^{17}\text{O}$ ) =  $9.30$  MHz and Behzadi *et al.* [13],  $\chi$  ( $^{17}\text{O}$ ) =  $8.87$  MHz. Several research groups have shown that  $^{17}\text{O}$  is

an effective probe to hydrogen bonding systems [29-33]. The differences in  $^{17}\text{O}$   $\chi, \eta$ s of the backbone are distinguishable between two conformers with and without influencing of the intramolecular hydrogen bond. The  $^{17}\text{O}$  backbone is very sensitive to structural changes between these two conformers,  $\Delta\chi_{\text{avg.}} = 0.45$  MHz,  $\Delta\eta_{\text{avg.}} = 0.14$ . Table 4 shows the calculated  $^{17}\text{O}$  NQR parameters of backbone in solution. It should be noted that the calculated difference in  $\chi$  between  $\alpha$ -helices and  $3_{10}$ -helix is approximately half a MHz ( $0.51$  MHz). Thus, the results reveal that separate signals resulting from two models will be experimentally recognizable in solution.

**Table 2.**  $^{14}\text{N}$  NQR parameters of peptide backbone of a solvated fragment of HRPII

Nuclei	$3_{10}$ -helix		$\alpha$ -helix		$ \Delta\chi ^{\text{MHz}}$	$ \Delta\eta $
	$\chi^{\text{MHz}}$	$\eta$	$\chi^{\text{MHz}}$	$\eta$		
N-Asp1	3.76	0.34	3.84	0.20	0.08	0.14
N-His2	3.81	0.44	3.92	0.38	0.11	0.06
N-His3	3.32	0.44	3.80	0.35	0.48	0.09
N-Ala4	3.81	0.38	4.0	0.23	0.19	0.15
N-Ala5	3.57	0.40	3.74	0.35	0.17	0.05
N-Asp6	3.52	0.47	3.62	0.38	0.10	0.09
N-Ala7	3.37	0.49	3.58	0.32	0.21	0.17
N-His8	3.29	0.48	3.47	0.40	0.18	0.08
N-His9	3.19	0.48	3.64	0.39	0.45	0.09
N-Ala10	3.33	0.47	3.70	0.36	0.37	0.11
N-Ala11	3.56	0.44	3.88	0.39	0.32	0.05
N-Asp12	4.02	0.45	3.79	0.40	0.23	0.05
N-Ala13	3.24	0.39	3.40	0.31	0.16	0.08
N-His14	3.38	0.48	3.58	0.39	0.20	0.09
N-His15	3.18	0.46	3.55	0.36	0.37	0.10
N-Ala16	3.34	0.48	3.88	0.31	0.54	0.17

**Table 3.**  $^{17}\text{O}$  NQR parameters of peptide backbone of a fragment of HRPII

Nuclei	$3_{10}$ -helix		$\alpha$ -helix		$ \Delta\chi ^{\text{MHz}}$	$ \Delta\eta $
	$\chi^{\text{MHz}}$	$\eta$	$\chi^{\text{MHz}}$	$\eta$		
O-Ala2	9.53	0.33	9.94	0.29	0.41	0.04
O-Thr3	9.37	0.32	9.74	0.34	0.37	0.02
O-Asp4	9.44	0.32	10.06	0.26	0.62	0.06
O-Ala5	9.20	0.32	9.79	0.25	0.59	0.07
O-His6	8.93	0.45	9.59	0.31	0.66	0.14
O-His7	9.09	0.32	9.46	0.30	0.37	0.02
O-Ala8	9.16	0.32	9.57	0.29	0.41	0.03
O-Ala9	9.12	0.36	9.41	0.32	0.29	0.04
O-Asp10	9.16	0.39	9.62	0.30	0.46	0.09
O-Ala11	9.06	0.35	9.53	0.30	0.47	0.05
O-His12	8.89	0.46	9.48	0.31	0.59	0.15
O-His13	9.03	0.34	9.36	0.32	0.33	0.02
O-Ala14	9.13	0.33	9.51	0.30	0.31	0.03
O-Ala15	9.13	0.36	9.44	0.31	0.31	0.05
O-Asp16	9.14	0.39	9.61	0.33	0.47	0.06
O-Ala17	9.10	0.35	9.49	0.30	0.39	0.05

**Table 4.**  $^{17}\text{O}$  NQR parameters of peptide backbone of a solvated fragment of HRPII

Nuclei	$3_{10}$ -helix		$\alpha$ -helix		$ \Delta\chi ^{\text{MHz}}$	$ \Delta\eta $
	$\chi^{\text{MHz}}$	$\eta$	$\chi^{\text{MHz}}$	$\eta$		
O-Ala2	8.78	0.51	9.47	0.36	0.69	0.15
O-Thr3	8.64	0.40	9.22	0.44	0.58	0.04
O-Asp4	9.03	0.43	9.62	0.31	0.61	0.12
O-Ala5	8.90	0.45	9.40	0.37	0.50	0.08
O-His6	8.74	0.53	9.38	0.40	0.64	0.13
O-His7	8.76	0.40	9.12	0.44	0.36	0.04
O-Ala8	8.68	0.41	9.20	0.37	0.52	0.11
O-Ala9	8.70	0.42	9.17	0.46	0.47	0.04
O-Asp10	8.81	0.48	9.30	0.40	0.49	0.08
O-Ala11	8.66	0.46	9.13	0.40	0.47	0.06
O-His12	8.34	0.52	9.08	0.41	0.70	0.11
O-His13	8.70	0.42	9.09	0.47	0.39	0.05
O-Ala14	8.73	0.46	9.11	0.40	0.38	0.06
O-Ala15	8.81	0.45	9.24	0.41	0.43	0.04
O-Asp16	8.67	0.44	9.21	0.39	0.54	0.10
O-Ala17	8.84	0.48	9.29	0.42	0.45	0.06

## Conclusion

The  $^{14}\text{N}$  and  $^{17}\text{O}$   $\chi, \eta$ s of backbone of a fragment of HRPII protein for  $3_{10}$ -helix and  $\alpha$ -helix are calculated both in the gas phase and in solution. The results confirm that, regardless of the medium being gas phase or solution, in general, the  $^{17}\text{O}$  NQR would be more efficient than  $^{14}\text{N}$  NQR in identifying the protein conformer. In conclusion, these results support the availability of DFT methods in determining local electrostatic properties such as EFG for proteins with different secondary structures. It encourages the future use of quantum chemical techniques where experimental results are difficult to obtain or we lack such results for challenging proteins like HRPII.

## Acknowledgements

This work was supported by Department of Basic Sciences, Faculty of Chemistry, Tarbiat Modares University, Tehran, Iran.

## References

- [1] E. Oldfield, *Phil. Trans. R. Soc. B*, **2005**, *360*, 1347-1361.
- [2] P. Jain, B. Chakma, S. Patra, P. Goswami, *BioMed Res.Int.*, **2014**, <http://dx.doi.org/10.1155/2014/852645>.
- [3] T.E. Wellems, R.J. Howard, *Proc. Natl. Acad. Sci U.S.A.*, **1986**, *83*, 6065-6069.
- [4] L.J. Panton, P. McPhie, W.L. Maloy, T.E. Wellems, D.W. Taylor, R.J. Howard, *Mol. Biochem. Parasitol.*, **1989**, *35*, 149-160.
- [5] <http://www.rcsb.org/pdb/home/home.do>.
- [6] C.Y.H. Chio, J.F. Cerda, H.-A. Chu, G.T. Babcock, M.A. Marletta, *Biochemistry.*, **1999**, *2* (38), 16916-16924.
- [7] E.L. Schneider, M.A. Marletta, *Biochemistry*, **2005**, *44*, 979-986.
- [8] C. Toniolo, A. Polese, F. Formaggio, M. Crisma, J. Kamphuis, *J. Am. Chem. Soc.*, **1996**, *118*, 2744-2745.
- [9] N. Greenfield, G.D. Fasman, *Biochemistry*, **1969**, *8*, 4108-4116.
- [10] N.H. Andersen, Z. Liu, K.S. Prickett, *FEBS Lett.*, **1996**, *399*, 47-52.
- [11] D. J. Sullivan, I.Y. Gluzman, I. Y., D. E. Goldberg, *Science*, **1996**, *271*, 219-221.
- [12] A.V. Pandey, H. Bisht, V.K. Babbarwal, J. Srivastava, K.C. Pandey, V.S. Chauhan, *Biochem. J.*, **2001**, *355*, 333-338.
- [13] H. Behzadi, M.D. Esrafil, D. van der spoel, N. Hadipour, G. Parsafar, *Biophys.Chem.*, **2008**, *137*, 76-80.
- [14] J. Tomasi, B. Mennucci, R. Cammi, *Chem. Rev.*, **2005**, *105*, 2999-3093.
- [15] M.J. Frisch, G.W. Trucks, H.B. Schlegel, G.E. Scuseria, M.A. Robb, J.R. Cheeseman, V.G. Zakrzewski, J.A. Montgomery, R.E. Stratmann, J. C. Burant, S. Dapprich, J.M. Millam, A.D. Daniels, K.N. Kudin, M.C. Strain, O. Farkas, J. Tomasi, V. Barone, M. Cossi, R. Cammi, B. Mennucci, C. Pomelli, C. Adamo, S. Clifford, J. Ochterski, G.A. Petersson, P.Y. Ayala, Q. Cui, K. Morokuma, D.K. Malick, A.D. Rabuck, K. Raghavachari, J.B. Foresman, J. Cioslowski, J.V. Ortiz, B.B. Stefanov, G. Liu, A. Liashenko, P. Piskorz, I. Komaromi, R. Gomperts, R.L. Martin, D.J. Fox, T. Keith, M.A. Al-Laham, C.Y. Peng, A. Nanayakkara, C. Gonzalez, M. Challacombe, P.M.W. Gill, B. Johnson, W. Chen, M.W. Wong, J.L. Andres, M. Head-Gordon, E.S. Replogle, J.A. Pople, *Gaussian 98*, revision A.7; Gaussian, Inc.: Pittsburgh, PA, **1998**.
- [16] A.D. Becke, *J. Chem. Phys.*, **1993**, *98*, 5648-5650.
- [17] C. Lee, W. Yang, R.G. Parr, *Phys. Rev. B*, **1988**, *37*, 785-789.
- [18] M. Mirzaei, N.L. Hadipour, *J. Comput. Chem.*, **2008**, *29*, 832-838.
- [19] M. Monajjemi, B. Honarparvar, S. M. Nasser, M. Khaleghian, *J. Struc.Chem.*, **2009**, *50*, 67-77.
- [20] K. Gotoh, T. Asaji, H. Ishida, *Acta Cryst.*, **2008**, *C64*, o550-o553.
- [21] H. Honda, *Molecules*, **2013**, *18*, 4786-4802.

- [22] J. N. Latosińska, J. Seliger, V. Žagar, D. V. Burchardt, *J. Mol. Model.*, **2012**, *18*(1), 11–26.
- [23] M. Faal, A. Shameli, E. Balali, M. Monfared, *J. Chem. Pharm. Res.*, **2016**, *8*(5), 644-650.
- [24] M.H. Cohen, F. Reif, *Solid State Phys.*, **1957**, *5*, 321.
- [25] E.A.C Lucken, *Nuclear Quadrupole Coupling Constants*, Academic: New York, **1969**.
- [26] P. Pyykkö, *Mol. Phys.*, **2001**, *99*, 1617-1629.
- [27] W.L. Jorgensen, J. Pranata, *J. Am. Chem. Soc.*, **1990**, *112*, 2008-2010.
- [28] M. Torrent, D.G. Musaev, K. Morokuma, S.C. Ke and K. Warncke, *J. Phys. Chem. B*, **1999**, *103*, 8618-8627.
- [29] A.Takahashi, S. Kuroki, I. Ando, T. Ozaki, A. Shoji, *J. Mol. Struct.*, **1998**, *442*, 195-199.
- [30] G. Wu, A. Hook, S. Dong, K. Yamada, *J. Phys. Chem. A*, **2000**, *104*, 4102-4107.
- [31] G. Wu, A. Hook, S. Dong, H. Grondey, *J. Am. Chem. Soc.*, **2000**, *122*, 4215-4216.
- [32] G. Wu, S. Dong, *J. Am. Chem. Soc.*, **2001**, *123*, 9119-9125.
- [33] G. Wu, S. Dong, *Chem. Phys. Lett.*, **2001**, *334*, 265-270.